Advanced light trapping management by diffractive interlayer for thin-film silicon solar cells

Philipp Obermeyer, Christian Haase, and Helmut Stiebig

Citation: Appl. Phys. Lett. **92**, 181102 (2008);
View online: https://doi.org/10.1063/1.2919727
View Table of Contents: http://aip.scitation.org/toc/apl/92/18
Published by the American Institute of Physics

Advanced light trapping management by diffractive interlayer for thin-film silicon solar cells

Philipp Obermeyer,[a] Christian Haase, and Helmut Stiebig
Institute of Energy Research-Photovoltaics, Forschungszentrum Juelich, D-52425 Juelich, Germany

(Received 7 January 2008; accepted 14 April 2008; published online 5 May 2008)

Thin-film silicon solar cells made of amorphous and microcrystalline silicon in tandem cell configuration enable high efficiency and low-cost production. Precise control of the absorption in each diode by a wavelength-selective and diffractive interlayer provides optimized current matching. For this purpose, intermediate reflectors with periodically textured interfaces are investigated. The propagation of electromagnetic waves is simulated using a three dimensional Maxwell solver which considers both near field and far field optics. Design rules for intermediate reflectors and textured interfaces are presented. © *2008 American Institute of Physics*.
[DOI: 10.1063/1.2919727]

Compared to single-junction thin-film silicon solar cells, multijunction cells more effectively utilize the irradiated solar energy spectrum due to the different semiconductor band gaps. In tandem configuration, the amorphous silicon (a-Si:H) top cell has a band gap (E_{gap}) of ~1.8 eV, and absorbs the short wavelength light, while the microcrystalline silicon (μc-Si:H) with E_{gap} of ~1.1 eV absorbs the light with longer wavelength. The low-cost approach for thin-film silicon solar cells is very sensitive to film thickness since the throughput increases with decreasing layer thickness. Thus, sophisticated light trapping is an essential requirement for the design of thin-film solar cells.[1,2] The use of intermediate reflector layers is a promising approach to control light in multijunction solar cells.[3–5] Apart from varying the thicknesses of the two absorber layers, it is also possible to adjust the current matching by integrating an intermediate reflector (IR). This is of special interest, because amorphous silicon films suffer from the Staebler–Wronski degradation. The degradation in cell efficiency under illumination is less pronounced for thinner absorber layers. Therefore, thinner a-Si:H top cell layers, in the range of 200 nm, are desired. The integration of an IR between the a-Si:H top cell and the μc-Si:H bottom cell increases the top cell short circuit current density. A rigorous analysis of the tandem cell structure has been performed to estimate the potential of IRs with different designs. For this purpose, the shape of the individual interfaces between the layers has been individually optimized.

Simulations are performed with the finite integration technique[6] (CST Microwave Studio®), which rigorously solves the Maxwell's equations on a three dimensional grid in the time domain method (transient solver). The material properties in the simulated unit cell are locally described by the permeability (μ), the permittivity (ε), and the conductivity (σ) following the geometry in the cell. Since these parameters are wavelength dependent, the spectrum is simulated in 161 steps with 5 nm variation in wavelength. The optical properties of a-Si:H, μc-Si:H, and the transparent conducting oxide (TCO) ZnO are determined by characterization of individual layers.[7] Illumination is performed by a plane wave boundary condition at the top of the multilayer cell under normal incidence and circular polarization. The absorption in each layer is calculated and the quantum efficiency and maximum short circuit current density are computed assuming perfect collection of generated carriers, i.e., every absorbed photon generates an electron-hole pair that contributes to the photocurrent. The Maxwell's equations computation include all the optical near field aspects. They are neglected in optical simulations based on the ray tracing approach that only considers far field properties. The results of our fundamental study help to explain thin-film optics and give alternatives to the common randomly textured solar cells concept.

The standard structure of a micromorph tandem cell (denoted as structure A), is composed of several stacked layers (Fig. 1). For better light in coupling a textured TCO is used as a front contact. The texture (interface 1) consists of pyramids (period of 1000 nm and height of 300 nm). The influence of the structure height and period on the wave propa-

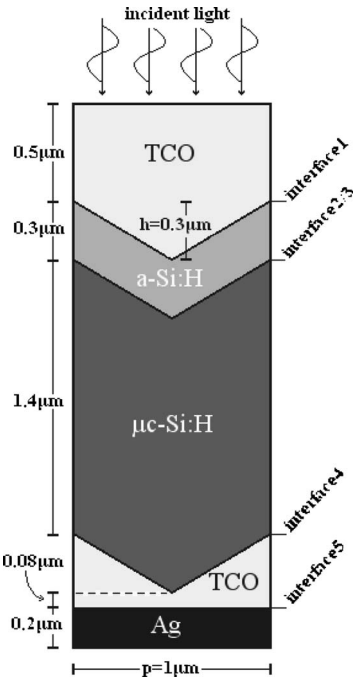

FIG. 1. Simulated unit cell (structure A).

[a]Electronic mail: philipp.obermeyer@gmx.de.

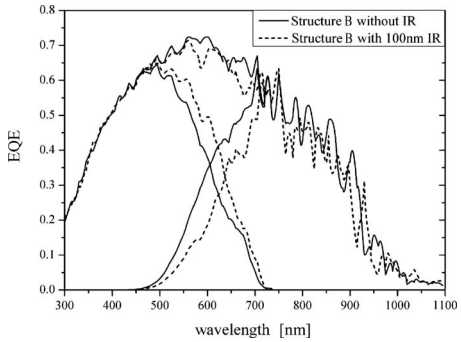

FIG. 2. Comparison of external quantum efficiency (for top, bottom, and total cells) with and without IR.

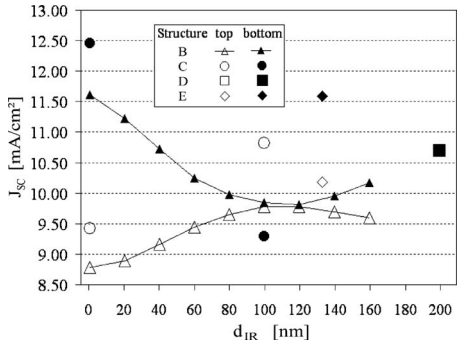

FIG. 3. Current density with varying reflector thicknesses.

gation within a single cell is discussed elsewhere in detail.[8,9] In the simulations, the front contact has a minimum thickness of 500 nm to maintain sufficient lateral electrical conductivity. Interfaces 2/3 are assumed to be conformal to interface 1. The highly reflective back contact consists of two layers: a silver layer of 200 nm and a TCO layer with a minimal thickness of 80 nm. The interface 5 between both layers is chosen to be flat because for periods of ~1000 nm this type of back reflector yields higher currents in the bottom cell.[8] The assembly consisting of a top cell of 200 nm thickness and an absorber layer thickness of the bottom cell of 1400 nm is denoted as structure A. Under illumination with an AM 1.5 spectrum the calculated short circuit current density (J_{sc}) for this structure is 8.8 and 11.6 mA/cm^2 in the top and bottom cells, respectively. Increasing the top cell thickness to 300 nm J_{sc}^{top} of 9.9 mA/cm^2 is found whereas J_{sc}^{bottom} slightly decreases to 10.5 mA/cm^2. Despite the thicker top cell, structure A is still limited by the top cell current.

To achieve current matching for a thinner top cell (d_{top} =200 nm) an additional TCO (ZnO) layer, called IR, is inserted between top and bottom cell. Every photon absorbed in the top cell instead of the bottom cell delivers ~60% more energy due to the reduced thermalization losses. This assembly is denoted as structure B. Figure 2 shows the external quantum efficiency (EQE) of this structure with and without IR. The insertion of a 100 nm thick reflector (dashed line) causes a considerable transfer of absorbed light from the bottom cell to the top cell in the spectral range between 480 and 720 nm, due to reflection at the IR. The amount of transferred current corresponds to 1.0 mA/cm^2 and results in J_{sc} of 9.8 and 9.85 mA/cm^2 for top and bottom cells, respectively. In this case, optimized matching conditions for a tandem cell structure are found. The total EQE is slightly reduced, especially for higher wavelength (λ) due to the parasitic losses (reflection at and absorption in the IR). On one hand, a photon with energy lower than the *a*-Si:H band gap can be reflected at the first encounter at the IR. On the other hand, it is possible for a photon of such energy to reach the bottom cell, and in this case the IR helps to trap it inside. Thus, it is difficult to distinguish between both effects, which also depend on the shape of the other interfaces. Also, absorption losses in the IR lead to a smaller red response. Therefore, J_{sc}^{bottom} nearly linearly decreases with IR thickness (~0.8 mA/cm^2 for 100 nm). The calculated EQE curve indicates the requirements for an optimized design of the IR. Its reflectivity should be high for 500 nm$<\lambda<$700 nm and low for higher λ. The reflectivity of an IR strongly depends on the thickness (d_{IR}) and is caused by an interference effect. This is confirmed by Fig. 3, which shows top and bottom cell currents as a function of d_{IR}. The current density in the top cell J_{sc}^{top} increases with d_{IR} while J_{sc}^{bottom} decreases. For $d_{IR}>110$ nm this tendency reverses. The variation in J_{sc}^{top} and J_{sc}^{bottom} is caused by the spectral shift of the maximum of reflection rather than a decrease in the amplitude. An optimized d_{IR} is between 100 and 110 nm. For a two-dimensional (2D) geometry with tilted interface, this maximum of reflection is determined by the interference condition $\lambda_{max}^{refl}=4n_{ZnO}d_{IR}\cos^2\alpha$, where $n_{ZnO}\approx 2$ is the refractive index and $\alpha\approx 31°$ is the inclination angle between the IR surface and the incoming plane wave. For an optimum J_{sc}^{top} and the corresponding d_{IR} of 110 nm this 2D interference condition predicts a wavelength of maximum reflection at $\lambda_{max}^{reft}=640$ nm. Therefore, reflections in this λ range generate the highest current in the top cell (Fig. 2). Since a thinner IR shifts this spectral range to lower wavelength and a thicker IR to higher wavelength J_{sc}^{top} decreases. Thus, the ability to reflect light within the cell at a certain λ requires a defined layer thickness. Another way to control the magnitude of reflection is to change the refractive index of the reflector (nd=const.[3]). The investigations have shown that an optimal reflector thickness is in the range of 70–110 nm. This is in accordance with other results.[4]

Next, the influence on the period size of the pyramid was examined. Variations of the period size of the unit cell shows that small periods result in good light in coupling but insufficient light trapping. For efficient red light scattering and trapping, periods at interfaces 3 and 4 with larger period size are required. Well directed light management can be carried out, because the scattering behavior and the light in-coupling behavior strongly depend on the lateral feature size. Therefore, an assembly was investigated using a texture with a small period at interface 1 and 2 and a larger period at interface 4. Since the refractive indexes of *a*-Si:H and μc-Si:H are similar, the scattering of light with longer wavelength is mainly introduced by the texture of the back contact (interface 4). The changes are addressed in structure C (similar to Fig. 4 but without IR). Interface 1 is defined by 4×4 pyramids with a period of 300 nm and a height of 200 nm. Interface 2/3 is again conformal to interface 1. The top cell thickness is kept constant at 200 nm. Interface 4 consists of a single pyramid with a period of 1200 nm and a height of 800 nm (texture scaled by a factor of 4), and interface 5 is again flat. The total μc-Si:H volume is kept constant. The calculated currents are 9.4 and 12.5 mA/cm^2 for the top and bottom cells, respectively. These values are significantly higher compared to structure B without IR (8.8 and

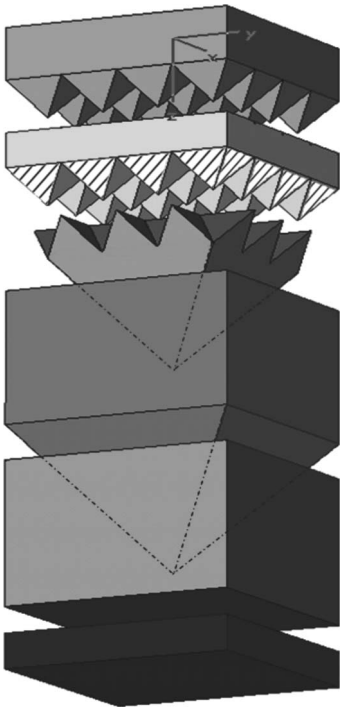

FIG. 4. Shape of the diffractive element in the unit cell (structure D).

11.6 mA/cm^2). Incorporating a conformal IR between interfaces 2 and 3 of 100 nm thickness in structure C leads to J_{sc}^{top} of 10.8 mA/cm^2 and J_{sc}^{bottom} of 9.3 mA/cm^2. For comparison, these values are also plotted in Fig. 3. In the latter case, the current of the tandem cell structure will be limited by the current from the bottom cell.

For single cells, a textured front contact shows an improved efficiency in comparison to cells with textured back reflector.[9] This effect can be used for the tandem structure by incorporating a diffractive IR (DIR) between the two absorbers. Since the DIR is discontinuous both absorbers touch each other at the hatched areas (see Fig. 4). The pyramid at interface 3 has a period of 1200 nm and a height of 800 nm and is therefore four times larger than the ones at interface 2. The resulting average thickness of the DIR is 200 nm. This assembly is referred to as structure D. Taking the preceding results into account, higher optical losses due to a thicker reflector are expected. However, the simulation shows the highest currents of 10.7 mA/cm^2 in the top and bottom cells. This additional gain in total current can be attributed to an interaction of the diffractive effects from the DIR and the textured back contact. Both are close to their optimum with a period size of 1200 nm. The J_{sc} of structure D is enhanced by 22% when compared to structure A and by 9.2% when compared to structure B with d_{IR}=100 nm. The special design of the DIR in structure D leads to lateral areas where the top and bottom diodes are separated by TCO and other lateral areas (hatched areas at interface 2) where no material with different refractive indexes between both diodes is incorporated. Depending on the number of pyramids used at interface 2 (2×2, 3×3, 4×4, and 5×5 pyramids) the uncovered area fraction (UAF) is 1/2, 1/3, 1/4, and 1/5, respectively. Thus, the property of the IR is also affected by the UAF. In structure D the UAF is equal to 1/4 and therefore, the reflectivity is slightly reduced. Nevertheless, the insertion of the modified DIR transfers 1.4 mA/cm^2 from the bottom cell to the top cell. Based on a detailed parameter study, the following equations roughly describe the influence of the top and bottom cell currents as a function of the grating parameter with respect to structure D (P_i=pyramid's period size at interface i, d_{IR}=thickness IR, UAF=uncovered area fraction),

$$J_{sc}^{top}(P_{1\&2},P_3,P_4,d_{IR},\mathrm{UAF}) = (20\,\%,<5\,\%,<1\,\%,15\,\%,15\,\%),$$

$$J_{sc}^{bottom}(P_{1\&2},P_3,P_4,d_{IR},\mathrm{UAF}) = (<10\,\%,15\,\%,25\,\%,20\,\%,5\,\%).$$

Another possibility to increase the initial J_{sc} is correlated to structure D with 3×3 pyramids at interfaces 1 and 2 which is denoted as structure E in the following. These pyramids have a period size of 400 mm and a height of 200 nm. Since the uncovered fraction of 1/3 is higher and the average thickness of the reflector is 133 nm less when compared to the previous structures based on a 4×4 pyramid array, the reflector does not shift sufficient current from the bottom to the top cell. In this case J_{sc}^{top}=10.2 mA/cm^2 and J_{sc}^{bottom} =11.6 mA/cm^2. It is not possible to increase the coverage fraction or average thickness without changing the whole fine-tuned system. To achieve current matching the top cell layer, thickness must be increased to 275 nm. In this case, current matching on a high initial level at 11 mA/cm^2 can be achieved. Compared to J_{sc} of structure A even with an increased top cell thickness of 300 nm a gain in current of more than 10% is found.

In summary, variations of the interfaces texture have been performed for the top and bottom cells. The conducted simulations show that single features cannot be independently optimized as their interaction determines the optical properties of the whole device. This fact makes the optimization of thin-film silicon solar cells more difficult. For a preferable a-Si:H top cell thickness of only 200 nm, period sizes of 300–400 nm for the top cell (interface 1) and 1200–1600 nm for the bottom should be considered. Based on a modified DIR design, a current gain of 20% compared to a structure without IR is predicted. The impact of individual texture parameters on the top and the bottom cell currents were presented to provide design rules for tandem cells with a diffractive interlayer.

[1] B. Rech, O. Kluth, T. Repmann, T. Roschek, J. Springer, J. Müller, F. Finger, H. Stiebig, and H. Wagner, Sol. Energy Mater. Sol. Cells **74**, 439 (2002).
[2] M. Vanecek, J. Springer, A. Poruba, O. Kluth, T. Repmann, B. Rech, N. Wyrsch, J. Meier, and A. Shah, *Proceedings of the 3rd WCPEC*, Osaka, Japan (IEEE, New York, 2003), p. 1527.
[3] K. Yamamoto, A. Nakajima, M. Yoshimi, T. Sawada, S. Fukuda, T. Suezaki, M. Ichikawa, Y. Koi, M. Goto, T. Meguro, T. Matsuda, M. Kondo, T. Sasaki, and Y. Tawada, Sol. Energy **77**, 939 (2004).
[4] D. Dominé, J. Bailat, J. Steinhauser, A. Shah, and C. Ballif, *Proceedings of the 4th WCPEC Conference*, Kona Island, Hawaii, USA (IEEE, New York, 2006), p. 1465.
[5] J. Krc, K. Brecl, F. Smole, and M. Topic, Sol. Energy Mater. Sol. Cells **90**, 3339 (2006).
[6] T. Weiland, Int. J. Numer. Model. **9**, 295 (1996).
[7] K. H. Jun, R. Carius, and H. Stiebig, Phys. Rev. B **66**, 115301 (2002).
[8] C. Haase and H. Stiebig, Appl. Phys. Lett. **91**, 061116 (2007).
[9] C. Haase and H. Stiebig, Prog. Photovoltaics **14**, 629 (2006).